

## Basics of Infrared Detection

Before the in-depth analyses of quantum well, ISBT, and QWIP – a specific infrared detector – we first discuss the general concept of how the temperature of an object influences the emission of infrared radiation, and how the detection of this radiation allows us to sense the temperature of this object. We also discuss the general properties of detector signal, noise, and figures of merit such as noise-equivalent power (NEP), detectivity, and noise-equivalent temperature difference (NETD).

### 2.1 Blackbody Radiation

To fully understand the process of infrared detection, we have to know some basic properties of the signals. The concept of temperature is equivalent to certain energy distributions. The Fermi–Dirac distribution describes the temperature of an ensemble of indistinguishable particles obeying the exclusion principle (fermions), e.g., of carriers in a semiconductor while the thermal energy distribution of particles with unlimited state occupancy (bosons) is given by the Bose–Einstein distribution function

$$f_{\text{B}}(E) = \frac{1}{\exp(E/k_{\text{B}}T) - 1}. \quad (2.1)$$

Here  $E$  is the energy,  $T$  is the temperature, and  $k_{\text{B}}$  is the Boltzmann constant.

This distribution function describes in particular the energy distribution of a photon field with temperature  $T$ . Applying (2.1) to the electromagnetic modes (photon states) in a cavity yields *Planck's radiation law*. In its commonly used form, it states that the *irradiance*  $\mathcal{I}_{\nu}$  (total power per unit surface area) at photon frequency  $\nu$  is given by [31]

$$d\mathcal{I}_{\nu} = \frac{2\pi h}{c^2} \frac{\nu^3 d\nu}{\exp(h\nu/k_{\text{B}}T) - 1}. \quad (2.2)$$

Here  $h$  is the Planck's constant which connects the frequency with the energy  $E = h\nu$  of a photon, and  $c$  is the speed of light. Equation (2.2) characterizes the radiation field inside a cavity with the radiation temperature  $T$ .

An important property of a thermal radiation field is that the radiation temperature is constant at each position inside the cavity. Considering now the walls of the cavity, thermal equilibrium can only exist if, at each part of the surface, the absorbed radiation power equals the emitted radiation power. The same is of course true for the surface of a small absorbing object inside the cavity. Consequently, at any frequency and incident angle, the emissivity  $\varepsilon$  of a surface equals the absorptivity (or  $(1 - \text{reflectivity})$  if the object is opaque).

Another important consequence of this concept is that the surface of an object with temperature  $T$  still emits radiation in the absence of incident radiation or, more generally, in the absence of thermal equilibrium between the object and the radiation field. For a given emissivity  $\varepsilon(\nu, \Omega)$ , the *radiance*  $\mathcal{H}_{\nu, \Omega}$  (radiation power per unit area and steradian) can be expressed as

$$d\mathcal{H}_{\nu, \Omega} = \varepsilon(\nu, \Omega) \frac{2h}{c^2} \frac{\nu^3 d\nu \cos \vartheta d\Omega}{\exp(h\nu/k_{\text{B}}T) - 1}, \quad (2.3)$$

where  $d\Omega = \sin \vartheta d\vartheta d\varphi$ .

In the simplest case, which is referred to as “blackbody,” the emissivity of the surface is  $\varepsilon = 1$ , such that the emitted radiation is identical to a thermal radiation field. Real objects often show a “greybody” behavior, where  $\varepsilon$  is constant with a value slightly less than one.

In general,  $\varepsilon$  can exhibit a complicated angular and frequency dependence. In particular, in the case of structured surfaces,  $\varepsilon$  may not just depend on the polar angle  $\vartheta$  but also on the azimuthal angle  $\varphi$ . Intentional modification of these dependencies can be achieved by applying appropriate coatings (reflection/antireflection) and by structuring the surface. Moreover, the reflectivity and thus also the emissivity are strongly affected if diffraction gratings are fabricated at the surface. In addition to diffraction, the emissivity is also influenced by surface plasmons, which can lead to a high degree of spatial coherence and narrow angular dependence of the emitted radiation [32].

For isotropic  $\varepsilon$ , integration of Eq. (2.3) over  $\vartheta$  and  $\varphi$  yields the total emitted power density per frequency interval, which has the same value as  $\mathcal{I}_{\nu}$  in (2.2) times an additional factor  $\varepsilon$ . Substituting for the photon energy  $E$  yields the power  $P_{\text{E}}$  per energy interval radiated from a surface with area  $A$ :

$$dP_{\text{E}} = A\varepsilon \frac{2\pi}{h^3 c^2} \frac{E^3 dE}{\exp(E/k_{\text{B}}T) - 1}. \quad (2.4)$$

Integration over the variable  $E$  (or  $\nu$ ) results in the Stefan–Boltzmann equation

$$P_{\text{tot}} = A\varepsilon\sigma T^4 \quad (2.5)$$

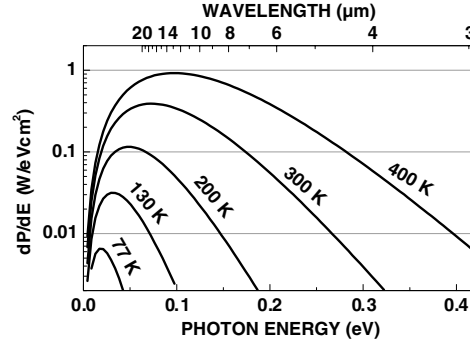


Fig. 2.1. Energy distribution of blackbody radiation vs. photon energy

with the Stefan–Boltzmann constant  $\sigma = 2\pi^5 k_B^4 / 15c^2 h^3 = 5.67 \times 10^{-8} \text{ W/m}^2 \text{ K}^4$ . According to Eq. (2.5), the total emitted radiation power density  $P_{\text{tot}}$  of a blackbody with  $\varepsilon = 1$  at 300 K equals  $46 \text{ mW cm}^{-2}$ .

The radiative energy distribution of a blackbody with  $\varepsilon = 1$  is shown in Fig. 2.1. Note that a different functional shape is obtained if the distribution is expressed as a function of the wavelength  $\lambda = c/\nu$ , since  $d\nu = d\lambda/\lambda^2$ .

The blackbody radiation incident onto a small detector with area  $A$  through an optical objective can be expressed in terms of the *f-number*  $F_{\#}$  of the objective, which is the ratio between its focal length  $f_L$  and the lens diameter  $D_L$ . We thus obtain  $\tan(\vartheta/2) = D_L/2f_L = 1/2F_{\#}$ , or  $\sin^2(\vartheta/2) = 1/(4F_{\#}^2 + 1)$ . The objective redirects the incident light emitted from a blackbody onto the detector, and it can be shown that the incident photon flux is the same as if the clear aperture of the lens itself were a blackbody with the same temperature. Integrating over the angular variables, (2.3) thus yields

$$dP_{\text{v,lens}} = A \frac{1}{4F_{\#}^2 + 1} \frac{2\pi h\nu^3 d\nu}{c^2 (\exp(h\nu/k_B T) - 1)}, \quad (2.6)$$

which determines the radiation power incident onto the detector. This equation provides the basis for calculating the temperature resolution later in this chapter. We note that  $\vartheta$  or  $F_{\#}$  also determine the optical field of view.

## 2.2 Signal, Noise, and Noise-Equivalent Power

We now assume that the power  $P_S$  of a *signal* with photon energy  $h\nu$ , which is equivalent to a photon number  $\Phi = P_S/h\nu$  per unit time, is incident on a photon detector with an area  $A$ . There is a probability  $\eta$ , also called the (internal) quantum efficiency, that an incident photon is absorbed in the detector and contributes to the signal current  $I_S$  that is flowing in the external circuit. The *photoconductive gain*  $g_{\text{photo}}$  is defined as the ratio between the

statistically averaged number  $\overline{n_x}$  of electrons that are collected in the external circuit and the average number  $\overline{n_{\text{det}}}$  of absorbed or detected photons,

$$g_{\text{photo}} = \overline{n_x} / \overline{n_{\text{det}}}. \quad (2.7)$$

Here the statistical average  $\bar{x}$  of a stochastic variable  $x$  denotes its average over a large set of samples, each with duration  $\tau_{\text{int}}$ .

$I_S$  can thus be expressed as  $I_S = e\eta g_{\text{photo}}\Phi$ . The responsivity  $\mathcal{R}$  is then defined as the ratio  $I_S/P_S$ , which leads to

$$\mathcal{R} = \frac{e}{h\nu} \eta g_{\text{photo}}. \quad (2.8)$$

In the case of a photoconductor,  $g_{\text{photo}}$  can be expressed as the ratio between the mean free path of the photoexcited carriers before recombination and the total thickness of the active region between the contacts; and, equivalently, as the ratio between the excited carrier lifetime and the total transit time. In the case of a photodiode, each detected photon contributes exactly one electron to the signal. The responsivity is thus given by (2.8) with  $g = 1$ , though the concept of gain is usually not applied to a photodiode. For both cases, we have implicitly assumed that  $\tau_{\text{int}}$  is much larger than the duration  $\tau_p$  of the signal pulses associated with individual detected photons. If  $\tau_{\text{int}}$  approaches  $\tau_p$ , then the signal (and also the noise associated with the signal) will depend on the sampling time and on the detection frequency. In the context of QWIPs, this case will be discussed in Chap. 10.

The *noise* associated with a stochastic variable is determined by its statistical properties. In mathematical terms, the noise associated with a stochastic variable  $x$  is given by its *variance*, defined by  $\text{var}(x) = \overline{(x - \bar{x})^2}$ .

In the case of a photodiode, each detected photon gives rise to a photocharge of exactly one electron. Thus, the number  $n_x$  of electrons collected during the sampling time  $\tau_{\text{int}}$  obeys a Poisson distribution, meaning that the probability  $p(n)$  of collecting  $n$  electrons is  $p(n) = (\overline{n_x}^n / n!) \exp(-\overline{n_x})$ . The variance for the specific case of a Poisson distribution is  $\text{var}(n_x) = \overline{n_x}$ .

The time-averaged current  $\bar{I} = e\overline{n_x} / \tau_{\text{int}}$  is associated with the (squared) noise current

$$i_n^2 = \text{var}(I) \quad (2.9)$$

which, in the case of a photodiode, gives rise to  $i_n^2 = e\bar{I} / \tau_{\text{int}}$ . In practice, noise is measured as a mean square current transmitted through a filter with an effective bandwidth  $\Delta f$ . It can be shown that the sampling or measurement time  $\tau_{\text{int}}$  is related to the bandwidth by

$$\Delta f = 1/2\tau_{\text{int}}. \quad (2.10)$$

The noise  $i_{n,s}$  associated with a Poisson distribution is called *shot noise*. According to the previous discussion, it can be written as

$$i_{n,s}^2 = 2e\bar{I}\Delta f. \quad (2.11)$$

For a given signal, shot noise yields the lowest noise level obtainable for any detector since there is a one-to-one correspondence with the noise already contained in the statistics of the incident photons themselves.

An “ideal” photoconductor exhibits a somewhat more complicated statistics, since the lifetime of photoexcited electrons obeys in turn a Poisson distribution. Assuming again  $\tau_{\text{int}} \gg \tau_{\text{p}}$ , the signal is thus composed of a sequence of short pulses that are Poisson-distributed in time, and their amplitudes also show a Poisson distribution. It can be shown that these statistics result in the following noise expression:

$$i_{\text{n,gr}}^2 = 4eg_{\text{photo}}\bar{I}\Delta f. \quad (2.12)$$

This expression can be understood by the argument (see Sect. 4.3) that both carrier generation and recombination are associated with Poisson distributions, each of which generates a noise contribution as in (2.11).  $i_{\text{n,gr}}$  is thus called *generation-recombination (g-r) noise*. We note that a “real” photoconductor may obtain additional noise contributions, attributable to, e.g., impurity levels, traps, or various scattering events including impact ionization [33,34].

We point out that, for an ideal photoconductor, currents induced by optically or thermally generated carriers and the associated g-r noise are by definition associated with the same gain. The index of  $g_{\text{photo}}$  will therefore be omitted in the present context. Due to the discrete microscopic structure of QWIPs, it will sometimes be necessary, however, to distinguish between the gains arising from the responsivity and the noise.

Noise is not only induced by the signal  $P_{\text{S}}$  itself, but also by a background power  $P_{\text{B}}$  originating, e.g., from objects adjacent to the signal source, stray light, or emission from the objective, and by the dark current  $I_{\text{dark}}$  of the detector. Assuming that  $I_{\text{dark}}$  is associated with the same noise behavior as the optically induced currents, which is usually a good approximation for most detectors, the resulting noise current is readily obtained by substituting  $I = \mathcal{R}P_{\text{S}} + \mathcal{R}P_{\text{B}} + I_{\text{dark}}$  into Eqs. (2.11) and (2.12). Depending on the relative magnitudes of  $\mathcal{R}P_{\text{S}}$ ,  $\mathcal{R}P_{\text{B}}$ , and  $I_{\text{dark}}$ , we then distinguish between signal-noise-limited, background-noise-limited, and dark-current-limited detection.

Assuming that the dark current is caused by thermal excitation, we define the *thermal generation rate*  $G_{\text{th}}$  (the number of thermally generated carriers per time and volume  $\mathcal{V}$ ).  $I_{\text{dark}}$  is thus expressed as

$$I_{\text{dark}} = egG_{\text{th}}\mathcal{V}. \quad (2.13)$$

In the case of QWIPs,  $G_{\text{th}}$  is obtained by spatial averaging over the detector volume. Background-limited (BL) detection thus refers to the situation that the optical generation rate induced by the radiation exceeds  $G_{\text{th}}$ .

The NEP is defined as the signal power needed to obtain a unity signal-to-noise ratio. Since the ratio between the signal power and the noise power equals the ratio between the squared currents, the NEP is determined by the

condition  $i_n^2 = \mathcal{R}^2 P_S^2$ , such that  $\text{NEP} = i_n/\mathcal{R}$ . For signal-noise limited (SL) detection, we thus obtain

$$(\text{NEP})_{\text{SL},s} = \frac{h\nu}{\eta\tau_{\text{int}}} = \frac{2h\nu\Delta f}{\eta} \quad (2.14)$$

in the case of a photodiode, and

$$(\text{NEP})_{\text{SL},\text{gr}} = \frac{2h\nu}{\eta\tau_{\text{int}}} = \frac{4h\nu\Delta f}{\eta} \quad (2.15)$$

for a photoconductor. Similarly, BL detection yields

$$(\text{NEP})_{\text{BL},s} = \sqrt{\frac{h\nu P_B}{\eta\tau_{\text{int}}}} = \sqrt{\frac{2h\nu\Delta f P_B}{\eta}} \quad (2.16)$$

in the case of a photodiode, and

$$(\text{NEP})_{\text{BL},\text{gr}} = \sqrt{\frac{2h\nu P_B}{\eta\tau_{\text{int}}}} = \sqrt{\frac{4h\nu\Delta f P_B}{\eta}} \quad (2.17)$$

for a photoconductor. In the dark-limited (DL) case, (2.13) gives rise to

$$(\text{NEP})_{\text{DL},\text{gr}} = \frac{h\nu}{\eta} \sqrt{4G_{\text{th}}\mathcal{V}\Delta f} = \frac{h\nu}{\eta} \sqrt{\frac{4G_{\text{th}}\mathcal{V}\Delta f}{\tau_{\text{int}}}}. \quad (2.18)$$

We point out that the NEP in (2.15), (2.17), and (2.18) is not influenced by the gain of the photoconductor.

### 2.3 Detectivity and Noise-Equivalent Temperature Difference

The *detectivity*  $D$  of a detector is defined as the inverse of NEP. In order to specify the performance of a detector, the *specific detectivity*  $D^* = D\sqrt{A\Delta f}$  is often used.  $D^*$  is the detectivity normalized with respect to the detector area and the bandwidth of the measurement. This definition leads to the general expression

$$D^* = \frac{R\sqrt{A\Delta f}}{i_n}. \quad (2.19)$$

For BL detection in the presence of the background photon flux density  $\Phi_{\text{B,ph}}$  (irradiance  $\mathcal{I}$ ), given by

$$\Phi_{\text{B,ph}} = \frac{P_B}{h\nu A} = \frac{\mathcal{I}}{h\nu}, \quad (2.20)$$

we thus obtain from (2.16) and (2.17) the specific detectivities

$$D_{\text{BL},s}^* = \sqrt{\frac{\eta}{2h\nu\mathcal{I}}} \quad (2.21)$$

and

$$D_{\text{BL},\text{gr}}^* = \sqrt{\frac{\eta}{4h\nu\mathcal{I}}}. \quad (2.22)$$

Equations (2.21) and (2.22) are sometimes referred to as the  $D^*$  of a photovoltaic and photoconductive detector, respectively.

In the DL case, (2.18) yields

$$D_{\text{DL},\text{gr}}^* = \frac{\eta}{h\nu\sqrt{4G_{\text{th}}L_{\text{Det}}}}, \quad (2.23)$$

where we have introduced the total thickness  $L_{\text{Det}} = \mathcal{V}/A$  of the photoconductor. Assuming that the detected radiation is absorbed with the penetration depth  $\alpha$ ,  $\eta$  is given by  $(1 - \exp(-\alpha L_{\text{Det}}))$ , and  $\eta$  is proportional to  $L_{\text{Det}}$  for small  $L_{\text{Det}}$ . Therefore, the ratio  $\alpha/G_{\text{th}}$  can be used as a figure of merit of the detector material. For larger  $L_{\text{Det}}$ , this figure of merit can still be used since  $D^*$  according to Eq. (2.23) has its maximum for  $L_{\text{Det}} = 1.26/\alpha$ , where it has a value of  $(0.31/h\nu)\sqrt{\alpha/G_{\text{th}}}$  [20].

As expected, the detectivities in Eqs. (2.21)–(2.23) are independent of the measurement bandwidth and detector area. More generally,  $D^*$  is a figure of merit that specifies any detector for which  $i_{\text{n}}^2$  is proportional to the detector area.

The NETD is defined as the temperature difference  $\Delta T$  at which the induced change  $\Delta P_{\text{B}}$  of the background power equals NEP, i.e.,

$$\text{NETD} = \frac{\text{NEP}}{dP_{\text{B}}/dT}. \quad (2.24)$$

We note that (2.24), if expressed in terms of signal electrons  $N_{\text{S}} = P_{\text{B}}\mathcal{R}\tau_{\text{int}}/e$  and noise electrons  $N_{\text{N}} = i_{\text{n}}\tau_{\text{int}}/e$ , is equivalent to the intuitive relation  $N_{\text{N}} = (dN_{\text{S}}/dT) \times \text{NETD}$ . The NETD is probably the most important figure of merit characterizing detectors and arrays used for passive infrared detection and imaging.

In order to keep the following discussion simple, we consider infrared detection within a narrow spectral band  $\Delta\nu$  around the detection energy  $h\nu$ . In addition,  $h\nu/k_{\text{B}}T$  is assumed to be large enough such that the Bose–Einstein distribution in Planck’s radiation formula can be approximated by a simple exponential. In this case, we obtain

$$\frac{dP_{\text{B}}}{dT} \approx \frac{h\nu}{k_{\text{B}}T^2} P_{\text{B}}, \quad (2.25)$$

or equivalently,

$$\frac{dN_{\text{S}}}{dT} \approx \frac{h\nu}{k_{\text{B}}T^2} N_{\text{S}}. \quad (2.26)$$

Equation (2.26) now allows us to relate thermal resolution to the signal-to-noise ratio

$$\text{NETD} = \frac{k_{\text{B}}T^2}{h\nu} \frac{N_{\text{N}}}{N_{\text{S}}}. \quad (2.27)$$

This means in particular that in order to achieve a certain NETD, the required signal-to-noise ratio is proportional to the detection wavelength.

Restricting the discussion to an ideal photoconductor as in Eq. (2.17), the NETD can now be expressed as

$$\text{NETD} = k_{\text{B}}T^2 \sqrt{\frac{2}{h\nu\eta P_{\text{B}}\tau_{\text{int}}}}. \quad (2.28)$$

Substituting for  $P_{\text{B}}$  the accumulated signal electrons  $N_{\text{S}}$  yields

$$\text{NETD} = \frac{k_{\text{B}}T^2}{h\nu} \sqrt{\frac{2g}{N_{\text{S}}}}. \quad (2.29)$$

To give a typical example, let us assume thermal detection within the spectral band from 8 to 9  $\mu\text{m}$  at 300 K radiation temperature using a detector with  $\eta = 10\%$  and  $A = 30 \times 30 \mu\text{m}^2$  through an  $F_{\#} = 2$  objective at an integration time  $\tau_{\text{int}} = 20$  ms. According to Eq. (2.6), we expect an incident power of  $P_{\text{B}} = 1.5$  nW, and Eq. (2.28) predicts  $\text{NETD} = 7$  mK. If  $g_{\text{photo}} = 1$ , the photo charge amounts to about  $N_{\text{S}} = 1.3 \times 10^8$  signal electrons. Since this number is already somewhat larger than the typical storage capacity of a readout integrated circuit, such an NETD is only achievable by increasing the storage capacity or by working at reduced noise levels, which is achievable for lower  $g_{\text{photo}}$ . We will come back to this point in Chap. 9.

Finally, it is worthwhile to take a closer look at the number of noise electrons  $N_{\text{N}} = i_{\text{n,gr}}\tau_{\text{int}}/e$ . To this end, we express Eq. (2.12) in terms of  $N_{\text{S}}$  and  $N_{\text{N}}$ , which yields

$$N_{\text{N}} = \sqrt{2gN_{\text{S}}}. \quad (2.30)$$

The above example then yields  $N_{\text{S}}/N_{\text{N}} = 8,000$  (see also (2.27)), which imposes additional harsh requirements on the readout noise and on other noise sources associated with the detection electronics. The difficulty arises from the necessity to resolve very small changes in the thermal background, which, according to (2.25), are as low as  $\Delta P_{\text{B}}/P_{\text{B}} = 1.3 \times 10^{-4}$  for  $\Delta T = 7$  mK.